ELSEVIER

Journal of Electroanalytical Chemistry 380 (1995) 1–6

JOURNAL OF ELECTROANALYTICAL CHEMISTRY

Cyclic voltammetry of Pd + D codeposition

S. Szpak [a,*], P.A. Mosier-Boss [a], S.R. Scharber [a,1], J.J. Smith [b]

[a] *Naval Command, Control and Ocean Surveillance Center, RDT&E Division, San Diego, CA 92152-5000, USA*
[b] *Department of Energy, Washington, DC 20585, USA*

Received 23 July 1993; in revised form 10 November 1993

ABSTRACT

Processes associated with the Pd + D alloy codeposition are examined by cyclic voltammetry. The voltammograms cover the potential range: +0.3 to –1.3 V (measured against an Ag/AgCl/KCl (sat) reference) and indicate that the partial current due to the Pd^{2+} ion reduction is diffusion limited at slow scan rates. Except for the significant increase in cathodic currents due to D_2O reduction at ca. –0.25 V which occurs on a freshly generated Pd surface, the shapes of the voltammograms marginally differ from those recorded in the absence of Pd^{2+} ions in the electrolyte phase. A discussion of the dynamics of the interphase is presented.

Keywords: Interphase dynamics; Cyclic voltammetry; Pd + D codeposition

1. INTRODUCTION

In earlier work [1] we constructed a model of the Pd|D_2O interphase wherein we defined a transfer zone λ^* consisting of two interdependent layers, i.e. λ_e which is located within the metal and in contact with λ_s in the electrolyte phase. These two layers interact with one another during the transfer of deuterium. The degree of their participation is dependent upon the applied potential and the solution composition. We concluded that the driving force acts across the interphase whose properties can be expressed as a function of composition and applied overpotential: $\lambda^* = f(c_1, c_2, ..., \eta$. In particular, as the overpotential η becomes more cathodic, negative charges accumulate in the interphase, resulting in an extension of the λ_e layer and a higher D^+ content within the subsurface layer. Furthermore, we observed that weakly adsorbed deuterium is sensitive to the surface-to-volume ratio while strongly adsorbed deuterium is only slightly affected. On this basis, we identified three energetically different states of deuterium residing within the interphase λ^* which, in turn, determine the boundary conditions for deuterium sorption. Of course, each of the energetically different states, when acted upon with the same driving force, exhibit different transport velocities.

In this paper, we examine the Pd + D codeposition process(es) by employing standard programmed perturbation of the interphase in the form of potential scanning. A gold substrate was used to assure containment of deuterium. Details of the experimental arrangement have been described previously [1].

*To whom correspondence should be addressed.
[1]Present address: San Diego Mesa College, San Diego, CA 92111, USA.

2. CODEPOSITION REACTIONS

The total current I associated with the process of Pd + D codeposition is divided into a contribution I_1 needed for the reduction of Pd^{2+} ions and a contribution I_2 needed for the evolution of deuterium from D_2O molecules:

$$Pd^{2+} + 2e^- \rightarrow PdI_1, E - E_{0,1}, \alpha_1 \quad \text{(I)}$$

$$D_2O + e^- \rightarrow D(a) + OD^- I_{2,1}, E - E_{0,2}, \quad \text{(II)}$$

$$D(a) + D_2O + e^- \rightarrow D_2 + OD^- I_{2,2}, E - E_{0,2}, \quad \text{(III)}$$

$$D(a) + D(a) \rightarrow D_2 \quad \text{(IV)}$$

$$D(a) \rightarrow D(l) \quad \text{(V)}$$

The kinetics of Pd^{2+} reduction are complex, involving a number of steps [2–4]; the path leading to the evolution of deuterium is equally complex [5]. The formulation of the kinetic expressions for a simple case of parallel non–interacting processes is discussed in detail by Bockris and Reddy [6] and summarized graphically in Fig. 1. The driving force for each partial reaction is given by $\eta = E - E_{0,n}$, n = 1, 2, ..., where E denotes the Galvani potential difference and $E_{0,n}$ are the respective equilibrium potentials. However, since the codeposited deuterium interacts with Pd to form an alloy, the reversible potentials $E_{0,1}$ and $E_{0,2}$ must be redefined. According to Gorbunova and Polukarov [7], there is a shift in $E_{0,n}$ in the positive direction by the amount $\Delta G/zF$ given by

$$\Delta G = \frac{X - 1}{X} U + RT \ln X \quad (1)$$

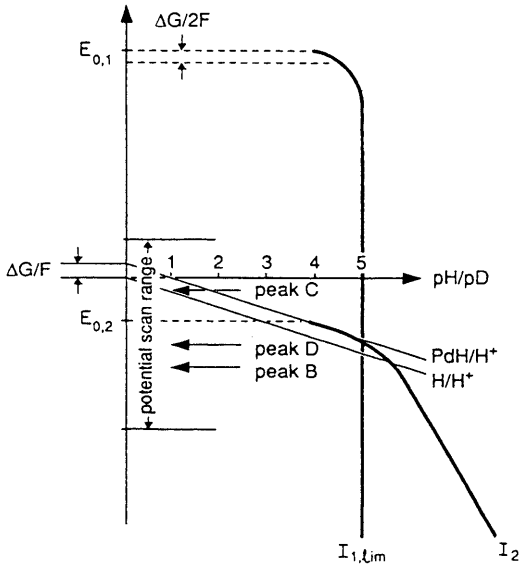

Figure 1. Representation of processes associated with Pd+D codeposition. Potential scan range and partial currents are superimposed on the Pourbaix diagram for the $H_2O + H_2$ system. ($I_{1,\,lim}$ refers to the rate of Pd^{2+} ion reduction and I_2 is a measure of D_2 generation).

Here, ΔG is the molar Gibbs energy of the alloy component in the alloy and U is the integral heat of formation of the alloy. In this expression, the first term represents the change in bonding energy and the second is the contribution due to a change in entropy. The total current is the sum of all the partial currents for eqns. (I)–(III):

$$j = \sum I_n \tag{2}$$

In what follows, we retain the independence of partial currents and correct for the Pd + D alloy formation by replacing the term $E_{0,n}$ appearing in the overpotential η with ($E_{0,n}$ $+ \Delta G/z_nF$). The form of the I_n vs. $E - E_{0,n}$ relation depends upon the experimental arrangement. For example, for slow scan voltammetry in the region under investigation, I_1 of eqn. (I) is expected to be diffusion limited while the current associated with the reduction of heavy water is controlled by the dynamics of the interphase.

3. EVOLUTION OF VOLTAMMOGRAMS

The effect of two factors on the evolution of the shape of voltammograms is considered, namely the number of cycles and the Pd^{2+} ion concentration.

3.1. Stabilization of voltammograms

Typical evolution of the voltammograms, covering the potential span –1.3 to + 0.3 V in which codeposition of Pd and D_2 takes place, is illustrated in Figs. 2 and 3 for two Pd^{2+} ion concentrations. Initially, during the negative scan, a featureless *I*–η relation with a substantial increase in cathodic current at potentials more negative than –1.0 V is recorded. On the return sweep, however, a cathodic peak appears at –1.0 V (peak A, insert to Fig. 2(a)) followed by a retracing of the negative branch until a potential of –0.60 V is reached. At somewhat more positive potentials, oxidation of weakly and strongly adsorbed deuterium occurs at –0.50 V and –0.05 V respectively. With subsequent scans, a shift of the entire voltammogram to more cathodic currents is observed. This is attributed to the continuous reduction of Pd^{2+} ions in the potential range + 0.3 to –1.3 V. Stabilization of the voltammograms coincides with the evolution of the electrode surface morphology. As the number of cycles increases, the electrode surface morphology evolves from that of dispersed individual crystallites to a fully developed porous surface. This is illustrated in Figs. 4(a), 4(b) and 4(c) which show scanning electron micrographs of the electrode surface after the first, third and sixth cycles. Evidently, the surface is morphologically fully developed after the sixth cycle. With further cycling, the surface area becomes larger and the Pd layer becomes thicker.

3.2. Effect of Pd^{2+} Ion Concentration

Four peaks are observed in the voltammograms which we refer to as A, B, C and D. Qualitatively, the scans in the positive direction are similar to those obtained in the absence of Pd^{2+} ions in the electrolyte [1]. As noted, the voltammograms shown in Figs. 2 and 3 are shifted in the negative direction. This shift is proportional to the Pd^{2+} ion concentration in the electrolyte phase. The effect of Pd^{2+} ion concentration is more evident in the negative scan. As shown in Figs. 2 and 3, the shape of the voltammograms is strongly dependent upon the Pd^{2+} ion concentration. In particular, peak A is present at low Pd^{2+} ion concentration and only appears during the first few cycles, and peak B is broader. Regardless of Pd^{2+} ion concentration, peak B encompasses the same potential range. With increasing cycle number peak B shifts to more positive potentials.

The effect of the solution composition on the shapes of peaks C and D is interesting. Initially, at low Pd^{2+} ion concentration, peak C consists of two closely spaced peaks which, with subsequent cycling, shift to more positive potentials and merge to form a single broad peak (Figs. 2(a) and 2(b)). At higher Pd^{2+} ion concentration, regardless of the cycle number, peak C is a superposition of two peaks which, however, remain at the same potential. In contrast, peak D exhibits different features, namely at low Pd^{2+} ion concentration it consists of two peaks D_1 and D_2, regardless of the scan

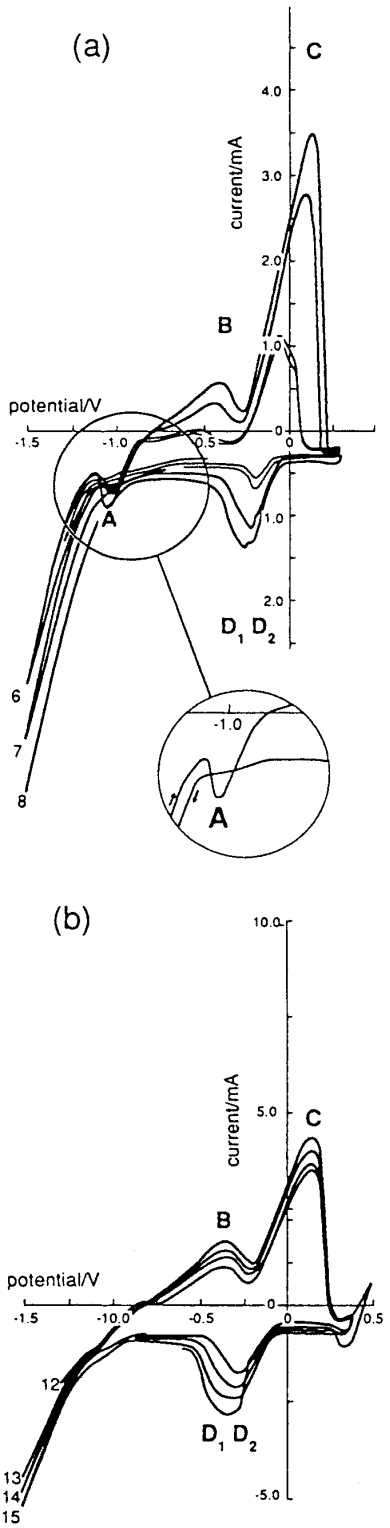

Figure 2. Evolution of the electrode response to potential scan: scan range, +0.3 to –1.3 V; scan number indicated; solution composition, 0.025 M $PdCl_2$ +0.3 M LiCl in D_2O. (a) Initial stage: scan numbers 6–8. The insert indicates current "cross-over" (scan direction indicated). (b) Voltammograms of morphologically fully developed working electrode: scan numbers 13–15.

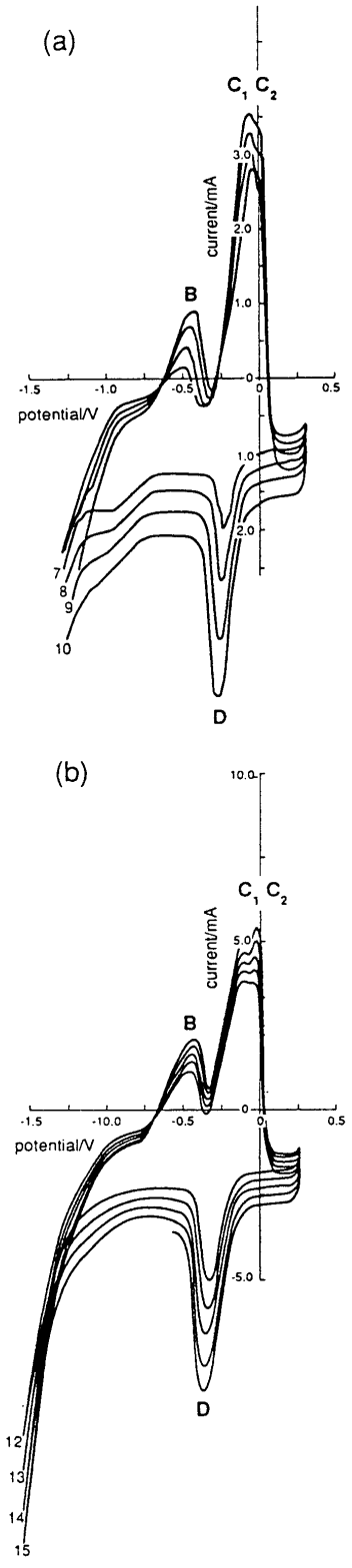

Figure 3. Evolution of electrode response to potential scan: scan range, +0.3 to –1.3 V; scan number indicated; solution composition, 0.05 M $PdCl_2$ +0.3 M LiCl in D_2O. (a) Initial stage: scan numbers 7–9. (b) Scan numbers 12–15.

number, while peak C remains a single peak (Figs. 3(a) and 3(b)). Furthermore, at high Pd^{2+} ion concentration, D is a single peak. It is noteworthy that at both high and low Pd^{2+} ion concentrations peak D shifts to more negative potentials during cycling and that the separation between peaks C and D decreases with increasing Pd^{2+} ion concentration.

4. QUALITATIVE INTERPRETATION OF VOLTAMMOGRAMS

In an attempt to determine the sequence of events and the magnitude of the processes associated with the codeposition of the Pd + D alloy via slow scan voltammetry, we assume that each partial current I_n in eqn. (2) is given by

$$\frac{I_n}{A(t)} = F\left[\sum_n D_n z_n \frac{\partial c_u}{\partial x} + \sum_m \Gamma_m \frac{d\theta_m}{dt}\right] \tag{3}$$

where $A(t)$ is the area of the charge transfer plane and Γ_m is the number of sites available for adsorption. The other symbols have their usual meaning. The first term on the righthand side represents the contribution due to diffusion while the second term is attributed to adsorption processes. The interpretation of the voltammograms is aided by Fig. 1, where the current–potential relations are superimposed upon the Pourbaix diagram for the E–H_2O system (the E–D_2O system is only slightly different). Owing to the low concentration of Pd^{2+} ions and the slow potential scan, I_l is assumed to be diffusion limited. Hence the first term on the righthand side of eqn. (3) can be regarded as a constant. Consequently, changes in the magnitude of current I are due to changes in surface coverage. Additionally, the shape of the voltammograms is affected primarily by the kinetics of adsorption. As indicated by eqns. (II)–(V) and discussed in ref. 5, the dependence of surface coverage on the electrode potential is complex.

In the context of Fig. 1, if $E_{0,2} < E < E_{0,1}$ only the reduction of Pd^{2+} ions is possible. As the electrode potential becomes more negative, i.e. when $E < E_{0,2}$, reduction of D_2O commences with the formation of a Pd + D alloy. The potential–independent cathodic current recorded for the potential range + 0.3 to ca. 0.0 V is in agreement with the assumption that the reduction of Pd^{2+} ions occurs at its limiting rate. Also, the continuous formation of a new surface is evident from the negative shift of the voltammograms.

4.1. Dynamics of the Interphase During Negative Sweep

A more detailed picture of the dynamics of the interphase during Pd + D codeposition is presented in Fig. 5 where the dominant fluxes consistent with the shape of the voltammogram are indicated. In particular, Fig. 5(a) defines specific regions of the potential scan where significant changes occur in the dynamics of the interphase. At equilibrium ($E = E_{eq}$) the composition of the interphase is such as to maintain equality of the chemical potentials with net zero fluxes across all segments of the interphase (Fig. 5(b)). However, as soon as the electrode is polarized, the composition of the interphase changes. In the potential range $E_{0,2} < E < E_{eq}$ the metallic Pd layer is deposited onto the $[D \cdots D]^+(\lambda^*)$ interphase

$$\begin{gathered} D^+(l) + D(\lambda_e) \\ \rightarrow [D \cdot \cdot \cdot D]^+(\lambda^*) + mPd^{2+}(\lambda_s) - 2me^-(\lambda_e) \\ \rightarrow Pd_{m-n}[D...D]^+(\lambda^*) + nPd(\lambda^*) \end{gathered} \tag{VI}$$

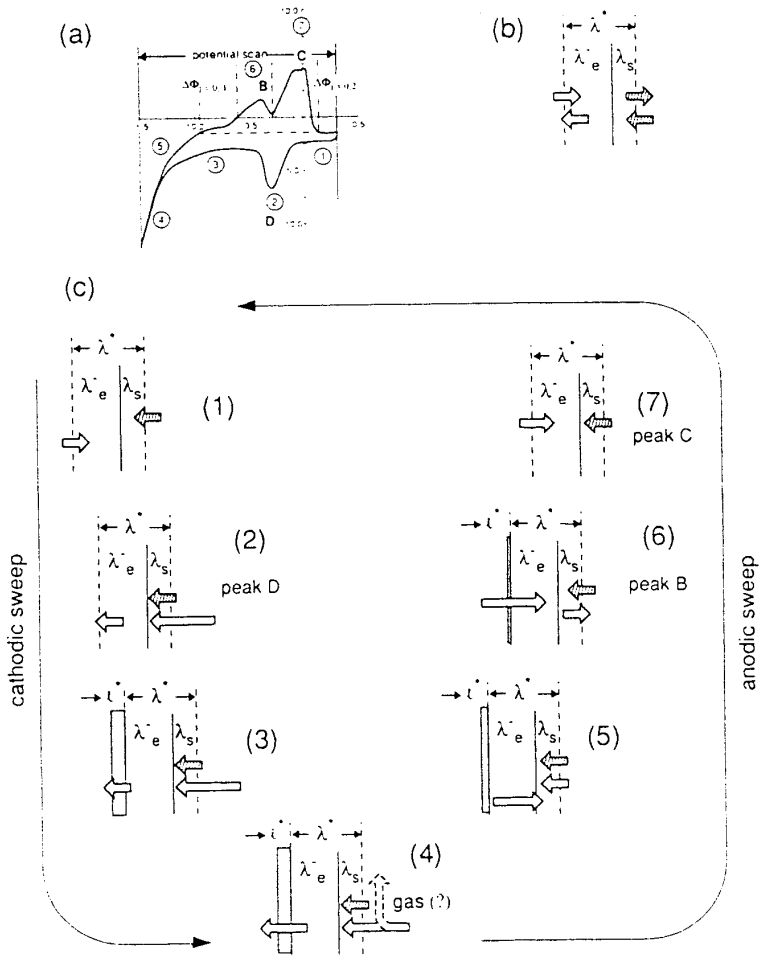

Figure 5. Dynamics of interphase: (a) regions of interest with regard to voltammogram; (b) fluxes and their magnitudes at equilibrium (rest potential); (c) fluxes and their relative magnitudes within regions defined in (a).

which, in turn, disturbs the interphase by redistributing the elements, as indicated by both the direction and length of the arrows in Fig. 5(c(1)). At this stage, the composition of the interphase is controlled by the rate of formation of the metallic layer and the transport of absorbed deuterium D(l) into the λ_e layer of the interphase. The freshly deposited Pd layer further modifies the interphase by restructuring the surface. The electrode response when E is only slightly more negative than $E_{0,2}$ (Fig. 5(c(2))) is of interest. At this point a significant increase in the cathodic current is observed (peak D) which is attributed to the high activity of the freshly prepared Pd layer, probably arising from surface restructuring and the creation of new adsorption sites. A direct consequence of the simultaneous rapid accumulation of sorbed deuterium in the λ_e layer and the deposition of metallic palladium is the formation of a thin layer 1* with a high D/Pd atomic ratio (Fig. 5(c(3))). This layer becomes part of the bulk electrode and represents a barrier for D transport because of the strong dependence of the diffusion coefficient on the D/Pd atomic ratio [8]. Symbolically, this situation is represented by

$$\begin{aligned} D^+(l) \leftrightarrow D^+(l^*) \rightarrow [D \cdot \cdot \cdot D]^+(\lambda^*) + mPd^{2+}(\lambda_s) \\ + nD_2O(\lambda_s) - 2(m+n)e^-(\lambda_e) \\ \rightarrow Pd_{m-n}[D \cdot \cdot \cdot D]^+(\lambda^*) + mPd(\lambda^*) + nOD^- \end{aligned} \qquad \text{(VII)}$$

The overlapping peaks D_1 and D_2 suggests a simultaneous filling of available sites which are energetically slightly different. Significant increases in the number of these sites results in a merging of peaks D_1 and D_2 present at higher Pd^{2+} ion concentration. With further polarization, e.g. when $E \ll E_{0,2}$, the dynamics of the 1nterphase changes, namely with an increase in the cathodic overpotential, the reaction path for deuterium evolution reaction changes [1,5]. We interpret this to conclude that the expanding electrode surface is saturated with deuterium, the amount of which is determined by the overpotential. Consequently, the excess of adsorbed deuterium may desorb into the gas phase (Fig. 5(c(4))).

4.2. DYNAMICS OF THE INTERPHASE DURING POSITIVE SWEEP

The events occurring on the return sweep, i.e. covering the potential region in the opposite direction, are illustrated in (Figs. 5(c(5))–5(c(7))). On the return sweep, the reduction of Pd^{2+} ions proceeds at the same rate $I_{1,lim}$, but the total cathodic current becomes less as the potential becomes more positive. In particular, within the potential range $E < E_{1=0,1}$ it is uncertain whether the decrease in cathodic current is due to a lower rate of deuterium generation or the oxidation of sorbed deuterons leaving the interphase region (Fig. 5(c(5))). However, as soon as the potential equals or exceeds $E_{1=0,1}$, i.e. when the cathodic current equals $I_{1,lim}$, oxidation of adsorbed deuterium commences resulting in peak B, and it terminates at $E_{1=0,2}$ (cf. Figs. 2 and 3). This situation is illustrated in Fig. 5(c(6)) and described symbolically by

$$D(a)(\lambda_e + OD^- - e^- \rightarrow D_2O \qquad \text{(VIII)}$$

This conclusion is supported by the slight displacement noted for higher Pd^{2+} ion concentration, as well as by the slight shift of peak B in the positive direction with increasing number of scans (cf. Figs. 2 and 3). The characteristic features of the voltammograms, namely coalescing and separating peaks (e.g. C and D) due to either scan number or Pd^{2+} ion concentration, reflect the cooperation between the participating processes and the properties of the electrodeposits. The dependence on the scan number enters via the evolution of electrode morphology modifying the local I–η distribution while the increased Pd^{2+} ion concentration changes the number of adsorption sites as well as the rate of growth of the Pd + D layer. The presence of energetically different adsorbed deuterium affects the transport across the interphase, resulting in the separation of closely spaced peaks. However, the coalescing of peaks indicates an increase in the concentration of one fraction of energetically different adsorbed deuterium.

It should be noted that, strictly speaking, the term “absorbed deuterium” includes the deuterium present in both the Pd bulk and the interphase λ_e. Furthermore, the Pd absorbed deuterium system results reversibly in the formation of α– and β–PdD. Cyclic voltammetry does not distinguish the processes by which the palladium deuterites are formed or decomposed nor those by which the bulk deuterium is transferred to the interphase region. In our discussion, “absorbed deuterium” refers to the deuterium present in the electrode interphase region. At this time, about all that can be said about the processes occurring within the bulk and at the bulk electrode interphase region is that, during the charging process, deuterium enters the electrode interphase through adsorbed states and then transits the electrode interphase into the bulk. On oxidation, a reverse process occurs in which the bulk absorbed deuterium enters the electrode interphase, subsequently leading to an unloading of the Pd. The mechanisms in Fig. 5(c) describe the processes occurring within the electrode and electrolyte interphase.

5. CONCLUDING REMARKS

(1) The existence of the double peaks C_1, C_2 on the positive scan and D1, D2 on the negative scan, observed at low Pd^{2+} ion concentration, and their locations are due to small differences in the respective transfer rates of energetically different adsorbed deuterium.

(2) The disproportionate increase in current at D corresponds to substantial absorption of deuterium by a freshly generated Pd surface. At more negative potentials, while the Pd reduction current continues at its limiting value (the actual current increases above the initial limiting value because of the increasing Pd surface area), the decrease in current indicates the formation of a thin layer l* which acts as a barrier, slowing the diffusion of interstitials.

REFERENCES

1. S. Szpak, P.A, Mosier–Boss, S.R. Scharber and J.J. Smith, J. Electroanal. Chem., 337 (1992)147,
2. M.F. Bell and J.A. Harrison, J. Electroanal. Chem., 41(1973)15.
3. J.A. Harrison, R.P. Hill and J. Thompson, J. Electroanal. Chem., 47 (1973) 431.
4. J.A. Harrison, H.B. Sierra Alcazar and J. Thompson, J. Electroanal. Chem., 53 (1974)145.
5. S. Szpak, C.J. Gabriel, J.J. Smith and R.J. Nowak. J. Electroanal. Chem., 309(1991)273.
6. J. O'M. Bockris and A.K.N. Reddy, Modern Electrochemistry, Vol. II, Plenum Press, New York, 1972, p. 1223.
7. K.M. Gorbunova and Yu.M. Polukarov in C.W. Tobias (Ed.). Advances in Electrochemistry and Electrochemical Engineering, Vol. 5, Interscience, New York, 1967.
8. J.O'M. Bockris, D. Hodko and Z. Minevski in T. Bressani, E. Del Giudice and G. Preparata (Eds.), The Science of Cold Fusion, Conference Proceedings, Italian Physical Society, Vol. 33, SIF. Bologna, 1991.